The hard ellipsoid potential model and the limit of rotational energy transfer in molecular collisions

Paras Mal Agrawal, Shashank Tilwankar, and Narendra K. Dabkara

Citation: The Journal of Chemical Physics **108**, 4854 (1998); doi: 10.1063/1.475895
View online: http://dx.doi.org/10.1063/1.475895
View Table of Contents: http://scitation.aip.org/content/aip/journal/jcp/108/12?ver=pdfcov
Published by the AIP Publishing

The hard ellipsoid potential model and the limit of rotational energy transfer in molecular collisions

Paras Mal Agrawal, Shashank Tilwankar, and Narendra K. Dabkara[a)]
School of Studies in Physics, Vikram University, Ujjain (M.P.) 456 010, India

(Received 7 October 1996; accepted 2 December 1997)

The effect of angular momentum conservation constraints on the limit of the rotational energy transfer (RET) in a diatomic molecule due to collisions with an atom has been investigated. The importance of the classical limit of the rotational energy transfer, $(\Delta E)_{\max}$, predicted by the hard ellipsoid potential model has been found such that it is comparable to a well known parameter $|\Delta E|^*$, given by the two-parameter power-gap (PG) ''law'' and the RET cross sections computed on the real potentials. Numerical equivalence of $(\Delta E)_{\max}$ and $|\Delta E|^*$ for various types of potential surfaces over a wide range of potential parameters, collision energy and the mass of the system has been verified. The feasibility of obtaining the difference of the semimajor and semiminor axes of the hard ellipsoid potential from the scattering data and the PG ''law'' has also been discussed. © *1998 American Institute of Physics.* [S0021-9606(98)01510-4]

I. INTRODUCTION

One of the important conclusions regarding the mechanism of rotational energy transfer (RET) in molecular systems is the observation that for a large number of systems angular momentum conservation limits the rotational inelasticity of the system, i.e., though the law of conservation of energy permits a higher amount of rotational energy transfer, angular momentum conservation constraints prevent such higher amount of RET. Dexheimer *et al.*,[1] as well as Agrawal *et al.*,[2,3] have quantitatively demonstrated such behavior, in agreement with the experiment, for a large number of systems by computing the limit of angular momentum transfer in terms of the product of collision time with the magnitude of the torque at the classical turning point.

Recently, McCaffery and his co-workers[4–6] explored various aspects of RET by treating the conversion of orbital angular momentum to the angular momentum of the molecule at the repulsive wall of an anisotropic intermolecular potential. Considering the total angular momentum, $\mathbf{J_T}$, as a sum of the orbital angular momentum, $\mathbf{r}\times\mathbf{p}$, and the angular momentum of the molecule, $\mathbf{J}$, the conservation of angular momentum can be expressed as

$$\mathbf{\Delta J_T}=\Delta(\mathbf{r}\times\mathbf{p})+\mathbf{\Delta}(\mathbf{J})=0, \tag{1}$$

which leads to

$$\Delta\mathbf{J}=-\mathbf{r}\times\mathbf{\Delta p}, \tag{2}$$

if $\mathbf{r}$ is treated as constant.

Following Bosanac,[7] Osborne and McCaffery[4] recently assumed the target as a hard-core ellipsoid[8–10] and computed the maximum possible value of $\mathbf{r}\times\mathbf{\Delta p}$ at the potential wall to arrive at the maximum limit of such angular momentum transfer in terms of the dynamical parameters, and temperature of the system.

It would be important to perform an elaborate test of the expression for the maximum limit of angular momentum transfer thus obtained. Such a test would be useful for the RET cross sections computed using realistic potentials. One more interesting point may be to study the abovementioned classical limit of the angular momentum transfer in quantum mechanical cross sections. Owing to quantum mechanical tunneling and the softness of the realistic potentials, one expects the probability of a rotational transition to be nonzero, even in the classically forbidden region predicted by Bosanac[7] as well as by Osborne and McCaffery[4] on the basis of the hard ellipsoid potential and Eq. (2). However, we shall see that the scaling and fitting ''laws'' [11–15] such as the power-gap ''law'' [14,15] will prove useful in separating the classically allowed and classically forbidden regions.

In this study, in addition to carrying out an elaborate test of the validity of the hard ellipsoid potential model and Eq. (2), we shall also reconfirm that the division between the classically allowed and forbidden transitions given by the power-gap ''law'' is excellent.

After reviewing the classical limit of the angular momentum transfer for the hard ellipsoid potential in the next section, we have described the method of computation of cross sections and the different types of potential energy functions employed in Sec. III. Using the RET cross sections so computed and the power-gap law,[15] the determination of the classical limit of the rotational energy transfer is then given in Sec. IV. The numerical results are finally presented, discussed, and summarized in Sec. V.

II. HARD ELLIPSOID POTENTIAL AND MAXIMUM RET

Bosanac[7] treated this problem in a general way by computing the angular momentum transfer as a function of the orientation of the molecule and the incoming atom. We present here a simplified treatment along those lines with our focus on the maximum limit of angular momentum transfer.

[a)]Current address: Department of Physics, Govt. P.G College, Neemuch (M.P.), India.

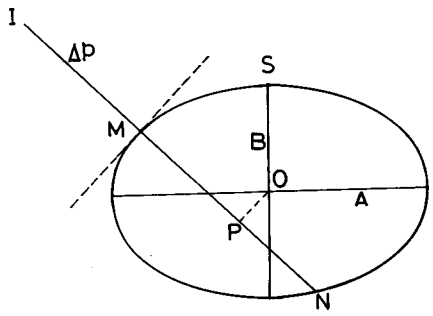

FIG. 1. A hard ellipsoid model of the rotationally inelastic atom–diatom collision.

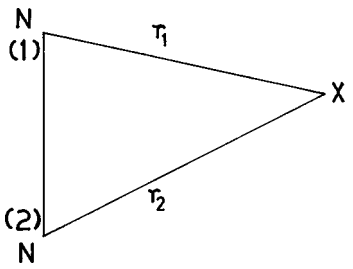

FIG. 2. Coordinates for the rigid rotor N_2-X system.

Figure 1 shows the hard ellipsoid potential seen by the incoming atom due to interaction with the diatomic molecule. The point O in the figure refers to the center of mass of the diatomic molecule.

The component of the linear momentum tangential to the ellipsoid is not altered by the collision. Therefore, the direction of change in momentum, $\mathbf{\Delta p}$, due to collision would be along the normal as shown by the line IM in the figure. For such a change in the linear momentum the magnitude of the conversion of the orbital angular momentum of the system into the angular momentum of the diatomic molecule given by Eq. (2) would be

$$\mathbf{\Delta J}=b_n|\mathbf{\Delta p}|, \tag{3}$$

where b_n is the length of the perpendicular OP on the normal IMN.

For the maximum possible value of b_n one can write following equation by using the properties of an ellipsoid:

$$(b_n)_{\max}=A-B, \tag{4}$$

where A and B are the lengths of the semimajor and semiminor axes, respectively.

For the maximum possible value of $\mathbf{\Delta p}$ one can write

$$|\mathbf{\Delta p}|_{\max}=\mathbf{p}-(-\mathbf{p}')=\sqrt{2\mu}(\sqrt{E}+\sqrt{E'}), \tag{5}$$

where μ is the reduced mass of the colliding system, and E and E' are the initial and final translational kinetic energies of the system, respectively. It is trivial to see that such extreme case of maximum momentum transfer would arise when the linear momentum, $\mathbf{p}'$, of the scattered atom is along the normal and is in the direction opposite to the incident momentum, $\mathbf{p}$.

Combining Eqs. (3)–(5), one can now write the following relation for the maximum classical limit of the angular momentum transfer:

$$(\mathbf{\Delta J})_{\max}=\sqrt{2\mu}(\sqrt{E}+\sqrt{E'})(A-B). \tag{6}$$

From this expression the limit of the rotational energy transfer in the molecule can be easily computed. For a simplest case, let us consider the diatomic molecule initially in the rotational ground state. The expression for the maximum amount of rotational energy transfer would be

$$(\Delta E)_{\max}=(\mathbf{\Delta J})^2_{\max}/2I$$
$$=(\mu/I)(A-B)^2(E+E'+2\sqrt{EE'}), \tag{7}$$

where I is the moment of inertia of the diatomic molecule.

Equation (7), together with the following energy conservation equation

$$E'=E-(\Delta E)_{\max}, \tag{8}$$

can be used to compute $(\Delta E)_{\max}$ from the knowledge of E, A, B, μ, and I.

III. COMPUTATION OF CROSS SECTIONS

A. Potential energy surface

For the computation of the cross sections, the diatomic molecule, N_2, is treated as a rigid rotor, and the interaction between the molecule and the atom, X, is taken as a pairwise sum of the spherical terms, i.e.,

$$V=V(r_1)+V(r_2), \tag{9}$$

where r_1 and r_2 are the $N^{(1)}$-X and $N^{(2)}$-X distances, respectively, as shown in Fig. 2.

For $V(r_i)$ the following general form of the Lennard-Jones (L-J) potential is taken with different values of n and m

$$V(r_i)=\varepsilon[\{m/(n-m)\}(r_0/r_i)^n-\{n/(n-m)\}$$
$$\times(r_0/r_i)^m], \quad (i=1,2), \tag{10}$$

where r_0 and ε are taken[16] as 3.60 Å and 2.328 meV for N-He and 3.63 Å and 5.352 meV for N-Ne, respectively.

The variation in the potential function is achieved by varying the values of n (=9, 12, 15, and 18) in Eq. (10), keeping $m=6$. Thus Eq. (9), together with Eq. (10), is used to obtain four varieties of potential functions which we shall denote as $V(n,m)$, i.e., $V(9,6)$, $V(12,6)$, $V(15,6)$, and $V(18,6)$. It is trivial to see that all these potentials have same location of minima, $r_i=r_0$, and the same value of the well depth, ε.

In addition to the abovementioned four sets of potential functions, potential functions having only repulsive terms have also been investigated. It would be convenient to denote such potentials by the notation $V_R(n)$. $V_R(n)$ has been obtained by deleting the attractive term from the potential $V(n,m)$.

B. Computation of cross sections

The integral inelastic cross sections (IICS) have been computed using the modified infinite order sudden approximation (IOSAM).[17] IOSAM cross sections, σ_{IOSAM}, are re-

lated to those calculated by the well known infinite order sudden approximation (IOSA), by the following relation:

$$\sigma_{\mathrm{IOSAM}}=(k_f/k_i)\sigma_{\mathrm{IOSA}}, \tag{11}$$

where k_f and k_i, respectively, represent the wave vectors corresponding to final and initial translational energies. Such a modification closes those channels which are not allowed by the energy conservation constraints.

The IOSA cross sections have been computed according to the formulation summarized in Ref. 18. For integration of Eq. (21) of Ref. 18, 100-point Gauss–Legendre quadrature has been used. Depending on the energy and the mass of the system N_2-X; the number of phase shifts have been varied in the range 100–400. The phase shifts have been computed using a 10-point Gauss–Mehler quadrature of the WKB phase shift equation as described by Pack.[19]

IV. THE POWER-GAP ''LAW'' AND THE CLASSICAL LIMIT OF RET

One of the popular forms of the scaling and fitting ''laws'' [11–15] that attempt to express a large number of cross sections in terms of a few fitting parameters is known as the power-gap ''law.'' [14,15] According to the power-gap ''law'' the cross sections, $\sigma(j_i\rightarrow j_f)$, can be expressed as:

$$\sigma(j_i\rightarrow j_f)=a(2j_f+1)(T_f/T_i)^{1/2}|\Delta E|^{-\gamma}, \tag{12}$$

where j_i and j_f are the initial and the final rotational quantum numbers; T_i and T_f, respectively, represent the initial and the final kinetic energy of the relative translational motion; and $|\Delta E|$ is the energy gap between initial and final rotational levels. a and γ are fitting parameters.

The dependence of a and γ on $|\Delta E|$ was first pointed out by Noorbatcha and Sathyamurthy.[15] By analyzing ten sets of data on CO_2-H_2, they found that for $|\Delta E|\leqslant|\Delta E|^*$ one set of parameters, a_{low} and γ_{low}, and another set of parameters, a_{high} and γ_{high}, for $|\Delta E|>|\Delta E|^*$ are needed to fit the data. It has also been noted that γ_{high} is a few times larger than γ_{low}. Several subsequent studies[2,3,20] observed the existence of such two regions. Schinke[20] pointed out that the transitions with $|\Delta E|\leqslant|\Delta E|^*$ corresponds to the classically ''allowed'' region and those with $|\Delta E|>|\Delta E|^*$ corresponds to the classically ''forbidden'' region.

Equation (12) yields the following equation that can be used to separate the two regions:

$$Y=-\gamma X+\ln a, \tag{13}$$

where

$$Y=\ln[\sigma(j_i\rightarrow j_f)(T_i/T_f)^{1/2}/(2j_f+1)], \tag{14}$$

and

$$X=\ln|\Delta E|. \tag{15}$$

Figure 3 gives a typical $X-Y$ plot that shows the existence of two straight lines signifying the two regions. The location of the critical point has been marked as $|\Delta E|^*$ in the figure.

For all sets of the computed cross sections, $|\Delta E|^*$ has been obtained by such plots. In view of the previous discussions $|\Delta E|^*$ has been treated as the classical limit of the rotational energy transfer, $(\Delta E)_{\max}$. In the next section we shall see that $(\Delta E)_{\max}$ so obtained by the power-gap ''law'' and the computed cross section is comparable to the $(\Delta E)_{\max}$ given by Eq. (7).

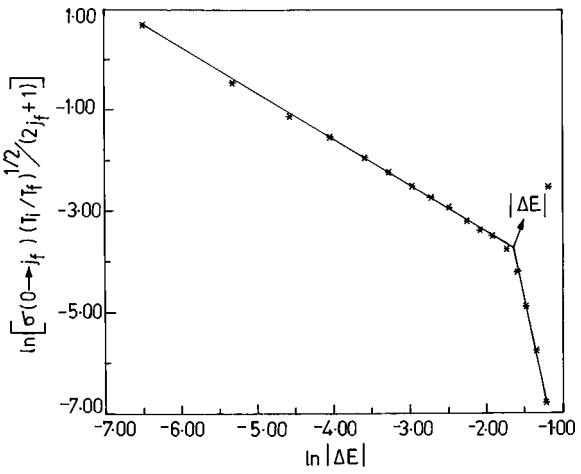

FIG. 3. $\ln[\sigma(T_i/T_f)^{1/2}/(2j_f+1)]$ vs $\ln|\Delta E|$ for $j_i=0$ at $E=0.3$ eV for N_2-Ne for the $V_R(9)$ potential.

V. RESULTS AND DISCUSSION

A. N_2-He and N_2-Ne

Table I lists the values of γ_{low}, γ_{high}, and $(\Delta E)_{\max}=|\Delta E|^*$ given by the power-gap ''law'' for the N_2-He system as a function of initial translational energy for different potentials. In all the calculations of cross sections, the molecule N_2 has been taken initially in the rotational ground state. The increase in $|\Delta E|^*$ with the increase in E is also clearly revealed by the plots shown in Fig. 4.

For comparison of $(\Delta E)_{\max}$ so obtained with the $(\Delta E)_{\max}$ predicted by the hard ellipsoid model the values of $(\Delta E)_{\max}$ given by Eq. (7) are also listed in the table. $(\Delta E)_{\max}$ so listed, in general, does not correspond to definite quantum levels. To translate the classical information contained in $(\Delta E)_{\max}$ into the quantum picture, the permissible (even) value of rotational quantum number, $(j_f)_{\max}$, corresponding to the rotational energy level just before the occurrence of classical rotational energy $(\Delta E)_{\max}$ is also listed in the table.

The values of A and B occurring in Eq. (7) have been obtained by assuming that the hard potential surface is represented by the classical turning point surface of the soft potential employed in the calculations of cross sections. The typical plots for a few values of energies E are as shown in Fig. 5 for the N_2-He system for the $V(12,6)$ potential. It is interesting to see that each surface is very close to an ellipsoid. The length of the semi-major and semi-minor axes of such an ellipsoid are identified as A and B, respectively. It may be mentioned that the semi-major axis of the ellipsoid has been observed along the direction of the molecular axis of the diatomic molecule, as shown in the figure. Typical values of A and B are 3.105 and 2.630 Å, respectively, for the $V(12,6)$ potential of the N_2-He system at $E=0.1$ eV.

TABLE I. Comparison of $(\Delta E)_{max}$ and $(j_f)_{max}$ values given by the hard ellipsoid model and those obtained by using the scattering cross sections and the power-gap ''law,'' for the N_2-He system.

Energy (eV)	γ_{low}[a]	γ_{high}[a]	$(\Delta E)_{max}$ (eV)		$(j_f)_{max}$	
			Scattering	Ellipsoid model	Scattering	Ellipsoid model
(a) Potential: V(12-6)						
0.10	0.85±0.11	6.84±0.58	0.033±0.003	0.032±0.003	10	10
0.15	0.81±0.07	8.10±0.53	0.049±0.003	0.048±0.004	12	12
0.20	0.80±0.05	8.39±0.56	0.064±0.003	0.064±0.005	14	14
0.30	0.82±0.04	9.16±0.52	0.097±0.004	0.097±0.008	18	18
0.40	0.79±0.02	8.02±0.64	0.119±0.005	0.130±0.011	20	22
0.50	0.79±0.01	6.72±0.061	0.141±0.005	0.163±0.014	22	24
(b) Potential: V_R(12)						
0.10	1.07±0.18	7.99±0.64	0.032±0.003	0.029±0.002	10	10
0.20	0.92±0.09	8.79±0.38	0.060±0.003	0.060±0.005	14	14
0.30	0.92±0.07	9.47±0.36	0.091±0.003	0.092±0.007	18	18
0.40	0.87±0.04	8.97±0.61	0.115±0.005	0.124±0.010	20	20
0.50	0.85±0.02	7.74±0.61	0.137±0.005	0.157±0.013	22	24
(c) Potential: V(18-6)						
0.10	0.73±0.08	6.21±0.54	0.034±0.003	0.034±0.003	10	10
0.20	0.78±0.08	8.69±0.54	0.074±0.004	0.069±0.006	16	16
0.30	0.78±0.06	9.42±0.53	0.110±0.004	0.104±0.010	20	18
0.40	0.74±0.03	8.02±0.59	0.134±0.005	0.140±0.013	22	22
0.50	0.72±0.02	6.59±0.56	0.157±0.005	0.176±0.017	24	26
(d) Potential: V_R(18)						
0.10	0.83±0.11	6.90±0.56	0.033±0.003	0.033±0.003	10	10
0.20	0.86±0.10	9.17±0.48	0.073±0.004	0.068±0.006	16	14
0.30	0.76±0.03	8.94±0.59	0.099±0.004	0.102±0.009	18	18
0.40	0.73±0.01	7.53±0.64	0.121±0.005	0.138±0.013	20	22
0.50	0.73±0.01	6.08±0.61	0.144±0.005	0.173±0.016	22	24

[a]The units of γ_{low} and γ_{high} are such that in Eq. (12) cross section is in $Å^2$ and ΔE is in eV.

The difference between the classical turning point potential surface given in Fig. 5 and the geometrical ellipsoid with the abovementioned values of A and B is very small. For example, the maximum value of $|R_e - R|$ is 0.0437 Å and the root mean square value of $(R_e - R)$ is 0.0267 Å, where R_e gives the distance between a point on the geometrical ellipsoid and its centre and R is the corresponding distance for the true classical turning point surface. The abovementioned data refer to the V(12,6) potential of the N_2-He system at $E = 0.5$ eV. For other values of energies the variation is still lower.

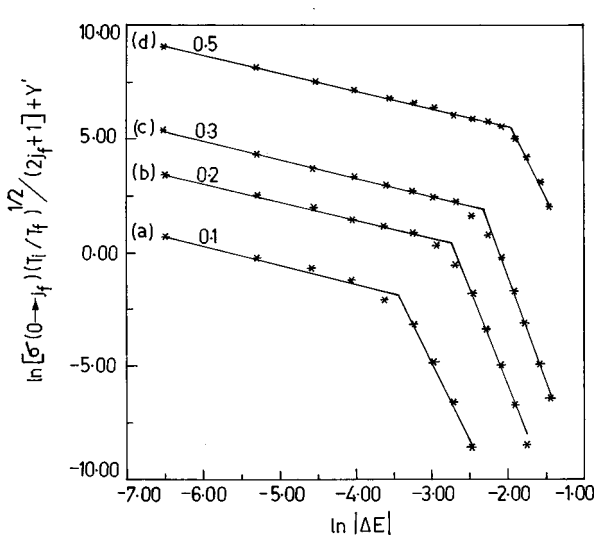

FIG. 4. $\{\ln[\sigma(T_i/T_f)^{1/2}/(2j_f+1)]+y'\}$ vs $\ln|\Delta E|$ for $j_i = 0$ for the N_2-He system. (a) $E = 0.1$ eV, $y' = 0$; (b) $E = 0.2$ eV, $y' = 3$; (c) $E = 0.3$ eV, $y' = 5$; (d) $E = 0.5$ eV, $y' = 9$. y' has been added just for the visual clarity.

A comparison of $(\Delta E)_{max}$ or $(j_f)_{max}$ given by the scattering data with the corresponding data obtained by the hard ellipsoid model shows that the two set of data listed in Table I are in very good agreement. An excellent agreement in $(\Delta E)_{max}$ values for the data corresponding to V(12,6)-0.2 eV, V(12,6)-0.3 eV, V_R(12)-0.2 eV, V_R(12)-0.3 eV, and V_R(18)-0.3 eV, and a perfect agreement in $(j_f)_{max}$ values for most of the sets are remarkable.

A similar trend of agreement can be seen in Table II for the N_2-Ne system.

It is interesting to look at the variation in γ_{low} and γ_{high} with energy as given in Table I. γ_{low} shows a nonmonotonic variation with E if standard errors are ignored. However, with the consideration of standard errors given in the table, one finds that γ_{low} is almost constant. The values of γ_{high}, however, show a different trend. The data reveal the existence of a maximum in the γ_{high} versus energy curve. The energy dependence of these parameters is a matter of further studies.

TABLE II. Comparison of $(\Delta E)_{max}$ and $(j_f)_{max}$ values given by the hard ellipsoid model and those obtained by using the scattering cross sections and the power-gap ''law,'' for the N_2-Ne system.

Energy (eV)	γ_{low}	γ_{high}	$(\Delta E)_{max}$ (eV)		$(j_f)_{max}$	
			Scattering	Ellipsoid model	Scattering	Ellipsoid model
(a) Potential: $V(12\text{-}6)$						
0.15	0.73	2.58	0.120	0.109	20	20
0.21	0.75	2.35	0.166	0.152	24	24
0.30	0.76	2.73	0.247	0.219	30	28
0.41	0.77	2.79	0.344	0.300	36	34
(b) Potential: $V_R(12)$						
0.15	0.83	4.52	0.099	0.101	18	18
0.20	0.83	4.08	0.137	0.136	22	22
0.30	0.84	4.86	0.223	0.207	28	28
0.40	0.85	4.53	0.309	0.279	34	32
(c) Potential: $V(9\text{-}6)$						
0.15	0.78	3.47	0.116	0.104	20	18
0.20	0.79	2.21	0.141	0.139	22	22
0.30	0.81	4.08	0.243	0.210	30	28
(d) Potential: $V_R(9)$						
0.15	0.94	6.74	0.091	0.089	18	18
0.20	0.92	5.59	0.116	0.121	20	20
0.30	0.92	6.90	0.193	0.187	26	26

B. Effect of mass

A comparison of the results for N_2-He and N_2-Ne given in Tables I and II demonstrates a mixed effect of the mass, r_0 and ε. For appreciating the effect of μ only, Table III gives the results for N_2-X having r_0 and ε values of the N_2-Ne system and the mass of X varying from 1.0 to 20.2 amu, at $E=0.15$ eV.

In addition to very good agreement between the $(\Delta E)_{max}$ values given by the scattering results and the ellipsoid model, one can see from Table III an increase in $(\Delta E)_{max}$ with the increase in mass of the atom X. This feature is very clearly shown by the plots in Fig. 6.

In this connection it would be interesting to discuss the effect of increasing $(\mu/I)(A-B)^2$ of the system that leads to an increase in $(\Delta E)_{max}$ according to Eq. (7). Equation (7) shows that for

$$(\mu/I)(A-B)^2=1,$$

one gets

$$(\Delta E)_{max}=E.$$

With a further increase in μ or $(A-B)$ such that

$$(\mu/I)(A-B)^2>1, \tag{16}$$

one can see that $(\Delta J)_{max}$ given by Eq. (6) would correspond to angular momentum transfer greater than that allowed by the energy conservation constraints (we are discussing the case in which the molecule is initially in the ground state). Therefore, such a change in the angular momentum can not occur. For a physical situation for which $b_n=(b_n)_{max}=(A-B)$ and condition (16) is satisfied, the value of $\mathbf{p}'$ in Eq. (5) would get adjusted such that $(\Delta E)_{max}$ cannot exceed E. Further, for such a system there would be many collisions such that b_n is lesser than $(b_n)_{max}$ given by Eq. (4), and $|\Delta p|$ is lesser or equal to $|\Delta p|_{max}$ given by Eq. (5) but their product may be such that $(\Delta E)_{max}=E$. Thus for the systems sat-

TABLE III. Comparison of $(\Delta E)_{max}$ and $(j_f)_{max}$ values given by the hard ellipsoid model and those obtained by using the scattering cross sections and the power-gap ''law,'' for the N_2-X systems, as a function of the mass of the atom X at collision energy $E=0.15$ eV. All other parameters of X are taken same as of Ne.

Mass of X (amu)	γ_{low}	γ_{high}	$(\Delta E)_{max}$ (eV)		$(j_f)_{max}$	
			Scattering	Ellipsoid model	Scattering	Ellipsoid model
1.0	0.95	5.92	0.014	0.015	6	6
4.0	0.91	8.86	0.057	0.047	14	12
12.0	0.73	4.96	0.096	0.090	18	18
16.0	0.74	4.04	0.113	0.101	20	18
20.2	0.73	2.58	0.120	0.109	20	20

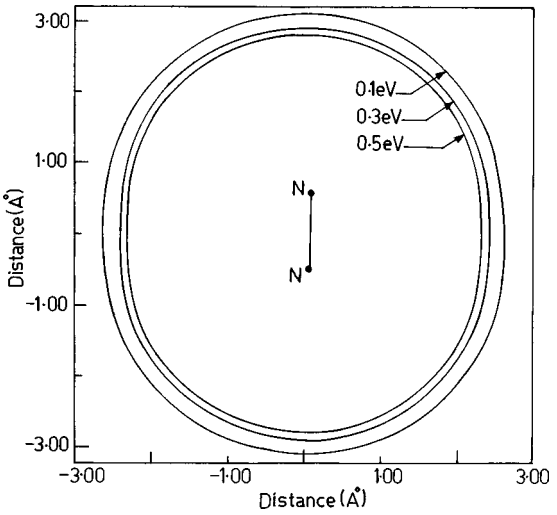

FIG. 5. The equivalent hard potential surfaces for N_2-He for the $V(12\text{-}6)$ potential.

isfying relation (16) the value of $(\Delta E)_{\max}$ would be equal to E. More about this point is being discussed in the subsection $E(i)$.

C. Effect of potential parameter r_0 and ε

The parameters A and B do not appreciably change with energy E. For example, for the $V(12,6)$ potential for the N_2-He system, A decreases from 3.105 to 2.760 and $(A-B)$ increases from 0.475 to 0.489 as E increases from 0.1 to 0.7 eV, respectively. Therefore, to study the dependence of $(\Delta E)_{\max}$ on $(A-B)$ as given by Eq. (7) we have varied the potential parameter r_0 from $0.5\,R_0$ to $1.5\,R_0$, where $R_0 = 3.595$ Å. The results so obtained for N_2-He at $E=0.1$ eV for the $V(12,6)$ potential are given in Table IV.

With such a change in the range parameter now A varies from 1.8274 to 4.3870 Å and $(A-B)$ varies from 0.601 to 0.394 as r_0 varies from $0.5\,R_0$ to $1.5\,R_0$, respectively. Thus the data presented in Table IV exclusively demonstrate the effect of variation of $(A-B)$ on $(\Delta E)_{\max}$. Here again we see that the agreement between the scattering results and that given by Eq. (7) is very good for $(\Delta E)_{\max}$ and is perfect for $(j_f)_{\max}$.

Unlike the effect of r_0, the parameter ε has a very small effect on $(A-B)$. Such an effect of varying ε from $0.5\,\varepsilon_0$ to $10.0\,\varepsilon_0$, where $\varepsilon_0 = 2.328$ meV, is shown in Table V for

TABLE IV. Comparison of $(\Delta E)_{\max}$ and $(j_f)_{\max}$ values given by the hard ellipsoid model and those obtained by using the scattering cross sections and the power-gap ''law,'' for N_2-He as a function of potential parameter, r_0, at collision energy $E=0.10$ eV.

			$(\Delta E)_{\max}$ (eV)		$(j_f)_{\max}$	
r_0/R_0	γ_{low}	γ_{high}	Scattering	Ellipsoid model	Scattering	Ellipsoid model
0.5	0.77	5.92	0.044	0.046	12	12
0.7	0.74	5.75	0.035	0.039	10	10
1.0	0.85	6.84	0.033	0.032	10	10
1.5	0.88	7.23	0.024	0.023	8	8

TABLE V. Comparison of $(\Delta E)_{\max}$ and $(j_f)_{\max}$ values given by the hard ellipsoid model and those obtained by using the scattering cross sections and the power-gap ''law,'' for N_2-He as a function of potential parameter ϵ, at collision energy $E=0.10$ eV.

			$(\Delta E)_{\max}$ (eV)		$(j_f)_{\max}$	
$\varepsilon/\varepsilon_0$	γ_{low}	γ_{high}	Scattering	Ellipsoid model	Scattering	Ellipsoid model
0.5	0.88	7.03	0.033±0.003	0.032±0.003	10	10
1.0	0.85	6.84	0.033±0.003	0.032±0.003	10	10
2.0	0.80	6.54	0.033±0.003	0.031±0.003	10	10
5.0	0.74	5.79	0.035±0.003	0.032±0.003	10	10
10.0	0.81	5.67	0.044±0.003	0.033±0.003	10	10

N_2-He at $E=0.1$ eV. Here $(A-B)$ only increases by about 2% as ε increases from $0.5\,\varepsilon_0$ to $10.0\,\varepsilon_0$. Accordingly, the value of $(j_f)_{\max}$ predicted by Eq. (7) remains unchanged. Table V shows that this value of $(j_f)_{\max}$ is in perfect agreement with that given by the scattering method.

For $\varepsilon = 10\,\varepsilon_0$, however, the difference in the $(\Delta E)_{\max}$ values is appreciable. It may be mentioned that for this set of computation the ratio of well-depth to the incident energy is 0.23. This suggests the possibility of larger departure for still larger well-depth. Such a departure is not unreasonable as Eq. (7) has been obtained for the perfectly hard potential.

D. Determination of $(A-B)$

One of the main advantages of the study of RET cross sections is to obtain the anisotropic intermolecular potential of the system. The inversion of the experimental cross sections to obtain the intermolecular potential has been a subject of considerable interest in recent years.[6,21–24] The validity of Eq. (7) for a large range of E, $(A-B)$, μ, r_0, and ε as observed here suggests the possibility of determination of $(A-B)$ from the knowledge of $(\Delta E)_{\max}$ provided by the analysis of scattering cross sections. Although such a determination of $(A-B)$ does not give the complete intermolecular potential, it is an important feature of the desired potential and can prove valuable in the determination of the potential surface.

For a comparison of $(A-B)$ value predicted by Eq. (7) with the actual value given by the potential, the results are presented for $V(9,6)$, $V_R(9)$, $V(15,6)$, and $V_R(15)$ potentials for the N_2-He system in the energy range 0.1–0.5 eV in Table VI. We see that the agreement is very good.

Using the results reported in Tables I–V one can also reanalyze the data to compare $(A-B)$ given by the potential with that obtained by using the scattering cross sections and the power-gap ''law.'' The degree of agreement would be better than that for $(\Delta E)_{\max}$ shown in those tables because of the fact that $(A-B)$ appears as $(A-B)^2$ in the expression for $(\Delta E)_{\max}$ in Eq. (7).

E. Other points

(i) Equation (7) can be rewritten as

$$-2\sqrt{EE'} = (E+E') - (\Delta E)_{\max}/Q, \tag{17}$$

where

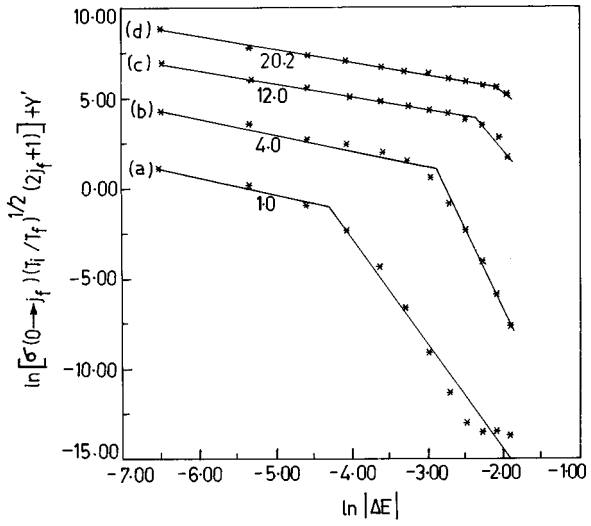

FIG. 6. $\{\ln[\sigma(T_i/T_f)^{1/2}/(2j_f+1)]+y'\}$ vs $\ln|\Delta E|$ for $j_i=0$ for the N_2-X system at $E=0.15$ eV. (a) Mass of X=1.0 amu, $y'=0.0$; (b) mass of X $=4.0$ amu, $y'=3.5$; (c) mass of X=12.0 amu, $y'=6.5$; (d) mass of X $=20.2$ amu, $y'=8.5$. y' has been added just for the visual clarity.

$$Q=(\mu/I)(A-B)^2. \tag{18}$$

Substituting the value of E' from Eq. (8) into Eq. (17), and then squaring both the sides, one can obtain the following equation on simplification:

$$(\Delta E)_{\max}=4EQ/(1+Q)^2. \tag{19}$$

Equation (19) is analogous to Eq. (4.6) of Bosanac,[7] and the same as Eq. (11) of Ref. 25. Apparently, for the computation of $(\Delta E)_{\max}$ it is easier to handle Eq. (19) than the numerical computation by using Eqs. (7) and (8). However, it can be seen that the value of $(\Delta E)_{\max}$ given by Eq. (19) is acceptable for $Q\leqslant 1$ only. For $Q>1$, the value of $(\Delta E)_{\max}$ given by Eq. (19) does not satisfy the original Eq. (7) or (17) from which Eq. (19) has been derived.

This anomaly is due to the fact that we have squared both sides of Eq. (17) to obtain Eq. (19). As such, Eq. (19) cannot distinguish minus or plus sign of the left hand side of Eq. (17), i.e., the following equation in place of Eq. (17) could also lead to Eq. (19):

$$+2\sqrt{EE'}=(E+E')-(\Delta E)_{\max}/Q. \tag{20}$$

We can further see that for $Q>1$ the value of $(\Delta E)_{\max}$ obtained from Eq. (19) satisfies Eq. (20) in place of Eq. (17). It may be added that Eq. (20) is not acceptable as it does not have any physical basis.

The physical situation and the value of $(\Delta E)_{\max}$ for $Q>1$ have already been discussed in detail just after Eq. (16). Equation (19), however, predicts $(\Delta E)_{\max}<E$ for $Q>1$.

In view of all these points it can be inferred that Eq. (19) is not acceptable for $Q>1$.

It may be mentioned that Eq. (19) has been treated applicable even for $Q>1$ in Refs. 7 and 25, without any consideration of the abovementioned points. As such, their results for $Q>1$ are to be reconsidered appropriately.

(ii) The deBroglie wavelength of the He atom at 0.1 eV is 0.45 Å. For Ne it is still smaller. The rotational energy spacing between the $j=0$ and 2 levels of N_2, 0.001496 eV, is very small compared to the lowest collision energy of the present studies. As such, the IOSAM formulation as well as the classical expression for the maximum limit of rotational energy transfer is found to work well here. For a system having large rotational spacings and large deBroglie wavelength it would be a matter of further research to investigate the importance of angular momentum constraints and the limit of the validity of Eq. (7). Further, the IOSAM may also be inappropriate for those systems and collision energies where the potential well depth is comparable with the collision energy. In all such cases the verification of Eq. (7) requires some more exact calculation of the cross sections.

TABLE VI. Comparison of $(A-B)$ values in Å given by the potential and those predicted by the scattering data for the N_2-He system.

Energy (eV)	γ_{low}	γ_{high}	$(A-B)$ Predicted	$(A-B)$ Potential
(a) Potential: V(9-6)				
0.10	0.95	7.30	0.484±0.022	0.450±0.017
0.20	0.88	8.58	0.469±0.011	0.455±0.018
0.30	0.90	9.52	0.474±0.010	0.459±0.018
0.40	0.86	8.68	0.452±0.010	0.462±0.019
(b) Potential: V_R(9)				
0.10	1.07	7.49	0.407±0.017	0.404±0.012
0.20	0.97	8.09	0.402±0.013	0.420±0.014
0.30	0.98	8.81	0.415±0.011	0.429±0.015
0.40	0.93	9.06	0.412±0.008	0.436±0.016
(c) Potential: V(15-6)				
0.10	0.78	6.51	0.491±0.022	0.475±0.021
0.30	0.76	8.83	0.489±0.010	0.479±0.022
0.40	0.74	7.45	0.464±0.010	0.480±0.022
(d) Potential: V_R(15)				
0.10	0.93	7.35	0.482±0.022	0.460±0.019
0.20	0.82	8.54	0.473±0.011	0.467±0.020
0.30	0.82	9.28	0.480±0.010	0.471±0.021
0.40	0.79	8.11	0.459±0.008	0.474±0.021

F. Summary

The effect of angular momentum conservation constraints on the limit of rotational energy transfer has been investigated. The classical limit of maximum rotational energy transfer has been reviewed for a hard ellipsoid potential model. The conversion of orbital angular momentum into the angular momentum of the diatomic molecule has been considered at the hard wall only.

The verification of the expression so obtained for the maximum amount of rotational energy transfer, $(\Delta E)_{\max}$, has been studied over a wide range of energies, potential functions and potential parameters. Corresponding to the classical limit $(\Delta E)_{\max}$ the final rotational quantum number $(j_f)_{\max}$ has also been computed in each case, considering the molecule initially in the ground state.

The $(\Delta E)_{\max}$ and $(j_f)_{\max}$ values predicted by the hard ellipsoid potential model are compared with those given by the computed cross sections. The two-parameter power-gap ''law'' has been used to compute $(\Delta E)_{\max}$ from the cross sections.

The systematic increase in $(\Delta E)_{\max}$ with the increase in the reduced mass of the system has been verified for N_2-X systems, where atom X has all properties of Ne except the mass which is taken as 1, 4, 12, 16, and 20.2 amu. The $|\Delta E|^*$ values given by the scattering results and the power-gap ''law'' are found to be in good agreement with the $(\Delta E)_{\max}$ values so obtained using the hard ellipsoid potential model.

Similarly, the dependence of $(\Delta E)_{\max}$ and $(j_f)_{\max}$ for N_2-He and N_2-Ne on the initial collision energy has been investigated for different types of potential surfaces over a wide range of potential parameters. In all cases it is found that the agreement between $(\Delta E)_{\max}$ and $|\Delta E|^*$ is good to excellent. The agreement, however, is not so good for the potentials having large well depth.

This study also suggests the feasibility of obtaining the difference of semimajor and semiminor axes, $(A-B)$, of the hard ellipsoid potential from the scattering data. For a few sets of computations, $(A-B)$ values so obtained are compared with those given by the actual potential. The agreement is found to be very good.

ACKNOWLEDGMENT

S.T. acknowledges the award of Junior Research Fellowship by C.S.I.R., New Delhi, India for pursuing this research.

[1] S. L. Dexheimer, M. Durand, T. A. Brunner, and D. E. Pritchard, J. Chem. Phys. **76**, 4996 (1982).
[2] P. M. Agrawal, N. C. Agrawal, and V. Garg, Chem. Phys. Lett. **118**, 213 (1985); *ibid.*, J. Chem. Phys. **83**, 4444 (1985).
[3] P. M. Agrawal and N. C. Agrawal, Chem. Phys. Lett. **122**, 37 (1985).
[4] M. A. Osborne and A. J. McCaffery, J. Chem. Phys. **101**, 5604 (1994).
[5] A. J. McCaffery, Z. T. Alwahabi, M. A. Osborne, and C. J. Williams, J. Chem. Phys. **98**, 4586 (1993).
[6] A. J. McCaffery and Z. T. Alwahabi, Phys. Rev. A **43**, 611 (1991).
[7] S. Bosanac, Phys. Rev. A **22**, 2617 (1980).
[8] D. Beck, U. Ross, and W. Schepper, Z. Phys. A **293**, 107 (1979).
[9] J. A. Serri, R. M. Bilotta, and D. E. Pritchard, J. Chem. Phys. **77**, 2940 (1982).
[10] F. A. Gianturco, J. P. Toennies, and M. Bernardi, J. Chem. Soc. Faraday Trans. **87**, 31 (1991).
[11] J. C. Polanyi and K. B. Woodall, J. Chem. Phys. **56**, 1563 (1972).
[12] B. J. Whitaker and Ph. Brechignac, Chem. Phys. Lett. **95**, 407 (1983).
[13] R. Ramaswamy, A. E. DePristo, and H. Rabitz, Chem. Phys. Lett. **61**, 495 (1979).
[14] T. A. Brunner, N. Smith, A. W. Karp, and D. E. Pritchard, J. Chem. Phys. **74**, 3324 (1981).
[15] I. NoorBatcha and N. Sathyamurthy, Chem. Phys. Lett. **79**, 264 (1981).
[16] (a) D. E. Gray, ed., *American Institute of Physics Handbook* (McGraw Hill, New York, 1957), p. 4.129. The geometric mean rule for ϵ and arithmetic mean rule for r_0 have been used. (b) R. A. Svehla, NASA Tech. Rep. **TR R-132** (1962).
[17] P. M. Agrawal and L. M. Raff, J. Chem. Phys. **74**, 3292 (1981).
[18] P. M. Agrawal and L. M. Raff, J. Chem. Phys. **75**, 2163 (1981).
[19] R. T Pack, J. Chem. Phys. **60**, 633 (1974).
[20] R. Schinke, J. Chem. Phys. **75**, 5205 (1981).
[21] S. D. Bosanac and N. Petrovic, Phys. Rev. A **41**, 5909 (1990).
[22] S. D. Bosanac and J. N. Murrell, J. Chem. Phys. **94**, 1167 (1991).
[23] J. C. Belchior, J. N. Murrell, and S. D. Bosanac, Chem. Phys. **176**, 155 (1993).
[24] J. C. Belchior and J. N. Murrell, J. Chem. Phys. **101**, 2016 (1994).
[25] See Ref. 10. The apparent difference in Eq. (19) of the present work and Eq. (11) of Ref. 10 is due to a minor typographical error.